EXPERIMENTAL AND THEORETICAL DEPOSITION PROFILES FOR STATIC AND DYNAMIC PCVD WITH WF6/H2 AND/OR ORGANOMETALLIC STARTING COMPOUNDS

G. Gärtner, P. Janiel, F. Weling

JOURNAL DE PHYSIQUE
Colloque C5, supplément au n°5, Tome 50, mai 1989

EXPERIMENTAL AND THEORETICAL DEPOSITION PROFILES FOR STATIC AND DYNAMIC PCVD WITH WF_6/H_2 AND/OR ORGANOMETALLIC STARTING COMPOUNDS

G. GÄRTNER, P. JANIEL and F. WELING

Philips GmbH Forschungslaboratorium Aachen, D-5100 Aachen, F.R.G.

Résumé

Les profils de dépôt obtenus en régime statique ou dynamique en CVD activé par plasma, à partir de WF_6/H_2 et/ou de Th-ß-dicétonate dans un mélange Ar / O_2 ont été investigés [1, 2]. Le plasma a été realisé par une décharge â courant continue entre une anode centrale mobile et le substrat cylindrique coaxial (cathode), dans un réacteur en quartz. Le but de ces activités est d'optimiser des structures de W dopé en ThO_2 pour le developpement de cathodes. Les profils d'épaisseur ou de concentration ont été ajustés avec une théorie établie pour le dépôt de SiO_2 dans un plasma microonde [3, 4, 5]. A partir de l'ajustement calculé en statique, les constantes de réactions bimoleculaires (10^{-15} a $3 \cdot 10^{-14}$ cm^3 /sec) ont été déduites la première fois pour les réactifs sus mentionnés (puissance de la decharge entre 107 et 310 Watt). En utilisant ces profils en statique, les profils en dynamique peuvent être prédits et comparés aux résultats experimentaux. Les critères d'obtention d'une concentration constante en dopant, d'une épaisseur constante, d'une composition determinée malgré le contenu de fluor et de carbone des réactants, sont discutés.

Abstract

Static and dynamic deposition profiles by plasma-activated CVD from WF_6/H_2 and/or Th-ß-diketonate starting compounds in an Ar/O_2 gas mixture [1, 2] have been investigated. The plasma was realized as dc glow discharge between a movable central anode and coaxially stacked substrate cylinders serving as cathode in a quartz reactor. The aim of these activities is to optimize e.g. ThO_2 doped W layer structures for cathode applications. Static and dynamic PCVD thickness or concentration profiles were then fitted to a theory formulated originally for SiO_2 PCVD with a microwave plasma [3, 4, 5]. From a computer fit of the static profiles, bimolecular reaction rate constants in the order of 10^{-15} to $3 \cdot 10^{-14}$ cm^3 /sec were determined for the first time for the above reactants (discharge powers between 107 and 310 Watt). Using the known static profiles, dynamic profiles can then be predicted and compared with the experimental results. Criteria for a constant dopant concentration and thickness region ("plateau") and for obtaining the right phase composition despite F-content and carbon-rich organometallic starting compounds are discussed.

Introduction

In order to carry out multi-component CVD of uniform layers on large substrates, plasma-activated CVD is one of the favourite methods. PCVD offers the advantages of similar deposition conditions for different components, high deposition rates and the accurate realization of prescribed concentration profiles. Yet there remains the problem of obtaining uniform deposits on larger areas, which is usually solved by using lower pressures (about 0.1 mbar), low mass flows and implies low efficiencies and low deposition rates. A better solution is to use dynamic PCVD instead of static PCVD by moving the deposition zone/ plasma periodically over the area where uniformity has to be obtained. This again works well for one component PCVD, but shows the additional feature of depth modulation of concentrations for multicomponent PCVD. If this has to be avoided, the remedy is a fast plasma movement together with a thermal treatment, leading to local interdiffusion of the components. Dynamic PCVD was first applied for the preparation of optical fibres [5, 6] by microwave plasma activated deposition of GeO_2/F doped SiO_2. Apart from this PCVD of insulators, a different technical approach had to be used for the deposition of layer structures

of metals doped (or mixed) with oxides for cathode applications. This has been realized by means of dc glow discharge activated CVD with periodic anode movement for the preparation of thoriated tungsten cylinders, which was already presented at Euro-CVD 6 [1]. A schematic view of the reactor is shown in fig.1 .

Nevertheless, the start for the prediction of concentration and thickness profiles under dynamic conditions are the static profiles. Moreover they offer the possibility to obtain total reaction rate constants for the plasma chemical reactions and circumvent the tedious theoretical calculations of taking into account all the different possible reaction paths. These bimolecular reaction rate constants were first obtained for SiO_2/GeO_2 deposition profiles by F.Weling, who formulated a theory for tubular reactors [3, 4]. Yet for the deposition of metals or metals doped with oxides, this procedure has not yet been carried out and no data were available up till now. Therefore W-, Th/W- and ThO_2-PCVD deposition profiles obtained in a static dc glow discharge were evaluated and fitted with the slightly modified computer-program originally developed by F.Weling for fits of static SiO_2/GeO_2 PCVD profiles [3, 4]. Plasma chemical reaction rate constants for WF_6/H_2-PCVD and $Th(tfa)_4/O_2$ PCVD are thus determined for the first time. With a further computer program also authored by F.Weling, dynamic profiles can then be predicted from the known static profiles.

Theoretical description of static PCVD profiles in tubular reactors

The tube in which the deposition takes place is divided into three zones (a schematic view is given in fig.2): a plasma zone of length L, the inlet and outlet sections in front and behind the plasma, respectively. The radius of the tube is a and cylindrical coordinates are used. Chemical reactions can only take place inside the plasma, but the molecules which are produced can diffuse into any of the three zones.
In order to apply this model also to the dc glow discharge activated deposition with a central anode as shown in fig.1, an effective radius a calculated from the open cross section is used. Since we use the simplification of plug flow as in [3] with constant gas velocity v, this further approximation is excusable. Axial or radial variations of power or electron density are not taken into account since they will only lead to local variations of the thickness profile in z-direction and won't influence the fitted parameters very much.
We will start the discussion with the formation mechanism of pure tungsten profiles. In this case the gas flow at the inlet is composed of WF_6/H_2 - typically in the ratio of 1 : 10 or even less - and Ar as an inert gas component. The overall reaction in the plasma leading to W deposition is given by

$$WF_6 + 3\,H_2 \rightarrow W\downarrow + 6\,HF\uparrow \qquad (1)$$

Since the W- profile is not significantly influenced by changes in the substrate temperature for plasma powers of the order of 200 Watt, we reason that the reaction is not surface induced. Therefore our model reaction is homogeneous, irreversible and of second order, if we take the initial reaction of WF_6 with H_2 as the rate limiting step. The last condition is not very stringent nor sensitive to the experiment, since in the experimental situation the hydrogen concentration is always much higher than the tungsten-hexafluoride concentration and we therefore get a pseudo-first order reaction independent of the actual reaction order. However, from the rate constant thus determined we can then calculate a bimolecular reaction rate constant. Finally there is the possibility to calculate an effective order from the concentration dependence at a more refined level. Since trimolecular reactions are unlikely due to the low probability of trimolecular collisions and since we have no WF_6 pyro- or plasmolysis (= unimolecular reaction), a bimolecular reaction gives the expected description of the process. The experimental results will later on give us hints where the model has to be refined and how the profile is possibly modified by reaction chains or power density gradients.
We will also regard the static PCVD reaction profiles of ThO_xF_y from Th-trifluoroacetylacetonate = $Th(tfa)_4$ / oxygen starting compounds and Ar and of simultaneous W/Th PCVD from a mixture

of the above source compounds. The simultaneous PCVD profile will be treated as a superposition of independent W and Th profiles in the first instance.

Therefore the following theoretical description is a more general one, where we start with a bimolecular reaction of the form

$$A\,R_1 + R_2R_3 \rightarrow A\,R_2\downarrow + (R_1R_3)\uparrow \qquad (2)$$

We then have the following rate equation inside the plasma zone

$$-\frac{d}{dt}[AR_1] = \frac{d}{dt}[AR_2] = k_0[AR_1][R_2R_3] \qquad (3)$$

From $[R_2R_3] \gg [AR_1]$,which is usually the case, it follows with $AR_1 =: \tilde{A}$, $AR_2 =: \tilde{B}$

$$-\frac{\partial n_{\tilde{A}}(\mathbf{r},t)}{\partial t}\bigg|_{chem} = \frac{\partial n_{\tilde{B}}(\mathbf{r},t)}{\partial t}\bigg|_{chem} = k n_{\tilde{A}}(\mathbf{r},t) \qquad (4)$$

where $\partial n/\partial t|_{chem}$ denotes the change of the concentration due to the chemical process and $k = k_0[R_2R_3]$ is the (pseudo-)first order reaction constant.
Once the $\tilde{B}$ molecules have been formed, they undergo axial and radial diffusion till they reach the surface of the tube where they form a deposit with a sticking probability about equal to 1 for the CVD cases discussed here.
The concentration n(**r** ,t) of particles diffusing in a flow of gas satisfies the equation of convective diffusion :

$$\frac{\partial n}{\partial t} + \mathbf{v}\cdot\mathbf{grad}\ n = D\Delta n + \frac{\partial n}{\partial t}\bigg|_{chem} \qquad (5)$$

The particle profile p(z) is defined as being the number of $\tilde{B}$ molecules arriving at the surface of the tube at a position z per second and per unit area

$$p(z) = -D\cdot\frac{\partial n_{\tilde{B}}}{\partial r}\bigg|_{r=a} \qquad (6)$$

Since an explicit deduction is given in [3], we here only give the final solution for the deposition profile:

$$p(z) = v\,n_{\tilde{A}}^0 \sum_{i=1}^{\infty} F_i \left\{1 - \exp\left[\frac{-(\lambda_i^+ + K/Pe)L}{a}\right]\right\} \times \exp\left(\frac{\lambda_i^+ z}{a}\right) \quad \text{if } z < 0,$$

$$p(z) = v\,n_{\tilde{A}}^0 \sum_{i=1}^{\infty} \left\{ -F_i \exp\left[-\frac{(\lambda_i^+ + K/Pe)L}{a} + \frac{\lambda_i^+ z}{a}\right] + G_i \exp\left(\frac{\lambda_i^- z}{a}\right) + (F_i - G_i)\exp\left(-\frac{Kz}{aPe}\right)\right\} \quad \text{if } 0 \le z \le L,$$

$$p(z) = v\,n_{\tilde{A}}^0 \sum_{i=1}^{\infty} G_i \left\{1 - \exp\left[-\frac{(\lambda_i^- + K/Pe)L}{a}\right]\right\} \times \exp\left(\frac{\lambda_i^- z}{a}\right) \quad \text{if } L < z \qquad (7)$$

with $\lambda_i^{\pm} = [Pe \pm (Pe^2 + 4\alpha_i^2)^{1/2}]/2 \qquad (8)$

and $F_i = \dfrac{2K(\lambda_i^- + K/Pe)}{Pe\,[(K/Pe)^2 + K - \alpha_i^2]\,(\lambda_i^+ - \lambda_i^-)}$, $\quad G_i = \dfrac{2K(\lambda_i^+ + K/Pe)}{Pe\,[(K/Pe)^2 + K - \alpha_i^2]\,(\lambda_i^+ - \lambda_i^-)}$, $\qquad (9)$

α_i are the zeros of the zero-order Bessel-function $J_0(\alpha_i\rho)$ and $n^0_{\tilde{A}}$ is the concentration of $\tilde{A}$ in the inlet region. The two dimensionless variables Pe = v/v_D and K = v_R/v_D are the Peclet-number and the Damköhler number K and characterize the PCVD process. It has to be noted that the efficiency of the process is measured by the quantity $\eta = kL/v$ where $\eta \gg 1$ implies total dissociation of the source compound AR_1. Using this equation, one can compute the thickness d(z,t) of the deposit at a point z after t seconds :

$$d(z,t) = p(z)\, M_{\tilde{B}}\, t \,/\, (N_A \cdot \rho_{\tilde{B}}) \qquad (10)$$

$M_{\tilde{B}}$ is the molecular mass of $\tilde{B}$ and $\rho_{\tilde{B}}$ its density; N_A is Avogadro's number.

Comparison with experiment and determination of reaction rate constants

a) Experimental results and parameters :

In the following section four experimental static PCVD-Profiles are evaluated, which are shown in fig. 3 - 6:
two W-deposition profiles obtained with differently shaped anode heads (fig. 3 and 4), a superposition of W and Th(O_xF_y) profiles from simultaneous Th/W PCVD (fig. 5a and 5b), and a Th(O_xF_y) profile obtained with $Th(tfa)_4/O_2$ starting compounds (fig. 6) only. The measured profiles are represented by dots (used for the computer fits) and thin lines in between, the thick solid curves are the results of the corresponding computer fit and will be discussed later on. Actually the experimental profiles have been corrected for constant density, since the deposited mass and not the deposited volume is the decisive parameter (see (6)).
For the computation of the deposition profiles several experimental parameters have to be known: The concentration $n_{\tilde{A}}$ is given by the ideal gas law as $n_{\tilde{A}} = P\, \dot{Q}_{\tilde{A}}/(\dot{Q}\, kT)$, where $\dot{Q}_{\tilde{A}}$ is the mass flow of $\tilde{A}$ at the inlet. The average gas velocity v is determined from the total flux $\dot{Q}$ by

$$v\,[cm/s] = \frac{T P_0 \dot{Q}\,[sccm]}{\pi a^2 T_0 P\, 60} \qquad (11)$$

T and P are the temperature and pressure inside the tube, P_0 and T_0 are the corresponding standard quantities. The length of the plasma zone can be determined e.g. by optical methods and amounts to 5 - 15 cm. Its accurate value is unimportant as long as $kl/v \gg 1$. Since in most cases accurate diffusion constants $D_{\tilde{B}\text{-}R_2R_3}$ are not known, they were calculated from molecular and atomic data using the modified hard core model results given by Dittmer [7] :

$$D[cm^2/s] = 4.65\ 10^{-4} \sqrt{\frac{M_{\tilde{B}} + M_{eff}}{M_{\tilde{B}} \cdot M_{eff}}}\ \frac{4}{(r_{\tilde{B}} + r_{eff})^2}\ \frac{T^{1.64}}{P}\ ;\ T < 2000K \qquad (12)$$

$r_{\tilde{B}}$ [Å] and r_{eff} [Å] are the diffusional radii of $\tilde{B}$ and R_2R_3 respectively. They can be determined for molecules with i atoms from $r = f_i\, S_{cov}$ where S_{cov} is the sum of the covalent radii of the two largest atoms plus the covalent radius of the next largest atom for $i > 2$ and $(f_1 \ldots f_7) = (1.4, 1.2, 1.0, 1.05, 1.1, 1.15, 1.2)$. The known experimental data are consistent with the D values thus obtained [7]. If there is a mixture of different gases as in our case, r_{eff} and M_{eff} are calculated according to

$$R_{eff} = \prod_i r_i^{x_i} \text{ and } M_{eff} = \prod_i M_i^{x_i} \qquad (13)$$

where x_i are the respective mole fractions.
In table I the experimental parameters used for the profile fits of fig. 3 - 6 are listed. z_A is the z-coordinate of the anode tip, which is correlated with the start of the plasma at z_0. Table II shows

the results of the computer fits for the reaction rate constants and the other relevant parameters. Actually in fig. 4 the diffusion constant has been fitted too, whereas the rate constant of table II was determined using the calculated D value. The experimental $d(z_i)$ profiles shown in fig. 3 to 6 were obtained from thickness d(z) measurements, which were in the case of density variations corrected by the weight gain g(z) results (not shown here) for each substrate cylinder of 27 mm length. The solid points were used for the profile fits. In the case of fig. 5 and 6 also concentration profiles had to be determined from SEM/EDAX measurements referenced to gauge samples. Above all in the less dense second deposition peak of fig. 6, the thickness values had to be reduced by using the weight values and assuming constant density along z direction, since p(z) in the fit represents the deposited mass profile ! Because the EDAX analysis besides Th and O also revealed a signficant F content, the density of $ThOF_2$ was used as an effective density in the cases of fig. 5b and 6 and yields good agreement between the d(z) and g(z) profiles in the first portion. For the evaluation of the depositions, the mass profile deposited on the anode in most cases was not taken into account (besides a multiplicative factor in some examples), since the weight ratio between the mass deposited on the cathode cylinders and the mass gain on the anode amounts to 2 : 1 to 3 : 1. Nevertheless, the mass gain on the anode must be considered when comparing the computed and experimental efficiencies. The anode profile contribution is of course not needed for the prediction of the dynamic cathode- d(z) profiles.
Fig. 7 shows a dynamic W PCVD profile obtained with an anode travel of 19 cm and an anode velocity of 38 cm/min. The total deposition time was 43 minutes, the other parameters correspond to the static W PCVD profile of fig. 3.

b) Results of Least-squares Fits and Discussion :

The results of the least-squares computer- fits of the static profiles are given in table II and are also depicted as thick solid curves in figs. 3 to 6. In fig. 6 the broken line represents the fit of the total profile (L = 17 cm) and the thick solid line the fit of the first deposition region only, which is reflected in a shorter adjusted length of the plasma zone of 10 cm. Actually more than the five static profiles shown here have been evaluated and the pertinent results will be also be considered for the general discussion. The parameters of a four parameter fit were : Diffusion constant D, decay length, shift z_0 (= begin of the plasma zone) and an effective deposition time t_{eff}. In fact only two fit-parameters are relevant, namely the decay length and L, since z_0 only represents an axial shift and D and t are essentially fixed. For the results of table II the diffusion constants were fixed to the the theoretical values, which are not very different from the fitted values. As a fifth (fourth) parameter, the length L of the plasma zone was also varied and the optimal values are listed in table II, since direct viewing is only possible through e.g. mesh substrates during the PCVD start. A further limiting condition imposed was the demand, that theoretical and experimental efficiencies should agree within the limits of cathode- and total efficiency, which is of course connected with the t_{eff}-value.

The comparison between experimental and theoretical profiles in figs. 3 to 6 may lead us to the conclusion, that theory and experiment do not match very well, since especially in fig. 6 there are strong discrepancies in the second portion, which have to be discussed. Yet a ± 30 % assigned uncertainty in the determination of the reaction rate constants also takes care of necessary improvements of the theoretical model. One has to bear in mind that no rate constants for the PCVD processes treated here were available up till now. Moreover, the procedure given here for obtaining the Damköhler number K and hence the rate constant from the static profiles is a straightforward one yielding a definite value which is consistent with the static PCVD profiles. The bimolecular reaction rate constants k_0 thus determined range from $1.4 \cdot 10^{-15}$ to $3. \cdot 10^{-14}$ and lie in the lower range of values given in the literature [3, 4, 8] for other reactions, which seems plausible for the normal dc glow discharge activation used here. The upper value results from further profile evaluations not contained in table II. Furthermore our bimolecular rate constant results from different static depositions for comparable gas mixtures are consistent with each other and imply a rate constant increase with increasing plasma power P_{pl}, which should be expected for

lower plasma powers. Based on an Arrhenius-type ansatz for the reaction rate, where the exponential term corresponds to the ratio of a free activation enthalpy to the electron temperature, which is again related to the discharge voltage divided by the total pressure, a quantitative extrapolation of ln k_0 against $1/P_{pl}$ yields rate constants of 3. to 6.$\cdot 10^{-14}$ cm^3/sec. This absolute limit is practically reached for plasma powers of about 1 kW. However, this power is not easily obtainable in the dc glow discharge case with a nearly current- independent power density and a length of the plasma zone which should not exceed about half the travel in the dynamic mode. Only a change of the accompanying gas admixture (e.g. Ar, O_2) could be the remedy. This is clearly demonstrated by the significant difference found between pure W PCVD and W PCVD simultaneously with metallorganic PCVD and oxygen admixture, where the W rate constant is much higher. This fact is very useful for dynamic PCVD tailoring, were the necessary length of the plasma zone and the anode travel is important for the length of the uniform deposition region. Despite these arguments in favour of the theoretical model, we will discuss possible sources of discrepancies in more detail in the following.

The first source for the differences obtained is the anode and the geometrical shape of the anode head. This is of course not yet taken into account in the theory and will yield locally different plasma densities, thus inducing an additional structure of the experimental profiles. This is clearly seen from the comparison of fig.3 and fig. 4. Yet the rate constants of the two W-PCVD profiles do not differ very much and the difference can be assigned to the small increase in discharge power. Of course an improved modified theory should also consider an inner cylinder surface contribution (anode), inferring at least one additional boundary condition in the model. The introduction of a plasma power density profile with additional fit variables may lead to a lower reduced χ^2, but will not necessarily help to clarify the plasma chemistry. Yet for the two independent fits of the Th/W PCVD profiles of fig. 5a, a two-step power density profile was assumed, defined by different z_0 and L and inspired by the fact that $Th(tfa)_4$ decomposition already takes place at lower plasma power densities.

A second question to be discussed is, whether the diffusion constants used here are really due to the diffusion of molecular species and not also of intermediates or of molecular clusters? It is well known that CVD reactions can also lead to homogeneous gas phase nucleation and cluster formation. Yet with the exception of the second downstream deposition peak of fig. 6 , the small variance of the freely fitted diffusion constants implies molecular diffusion, maybe with an additional contribution of two- or three-molecule clusters. Only in the case of $Th(O_xF_y)$- PCVD of fig.6, the second deposition peak with rather low mass density gives a clear hint for molecular cluster contribution. If this peak is fitted independently, the other parameters taken from the fit of the first peak, an effective diffusion constant for $\widetilde{B}$-clusters can be determined, inferring a mean molecule number of about 1000. A small cluster contribution is nearly always found in the downstream deposition region and can only be avoided by applying higher discharge power densities. This is however not freely adjustable for the normal dc glow discharge. Yet the simultaneous Th/W PCVD of fig. 5 shows the advantageous feature, that a second Th-containing less dense cluster peak is not present and hence also dense dynamic profiles can be obtained.

Another problem which can be derived from the static multicomponent PCVD results is the adjustment of the solid phase composition. In the case of preparation of thoriated tungsten cathodes by PCVD [1,2], which of course has been done in the dynamic mode for obtaining uniform deposits, the codeposition of F has to be avoided, but C-Content is favourable for cathode applications. Hence in this case, after each deposition pass a sweep with an intermediate Ar (Ar/O_2) plasma treatment is inserted, whereby a strong F-reduction is caused. Thus a composition of $W/W_2C/ThO_2$ is obtained. Of course a depth concentration modulation is also effected, since the deposition maxima of Th and W are spatially separated from each other and thus a sublayer structure with Th- and W-rich layers is induced. Obviously the cathode activation at 2000 K will lead to interdiffusion, but also a higher spatial depth modulation frequency by faster anode movement can be favourable.

Conclusion

By evaluation of static PCVD profiles, bimolecular reaction rate constants for W-PCVD and Th(O_xF_y)- PCVD and for simultaneous Th/W PCVD have been determined for the first time, which are consistent with other plasma-assisted processes. The theory of F.Weling also gives a good overall description of the dc glow discharge activated CVD despite the absence of an anode contribution, which has to be accounted for in a more refined theory. However it can be clearly seen, that the detailed evaluation of these static profiles offers a new tool for plasma assisted process diagnostics. The static profiles are also prerequisites for the dynamic profile tailoring in order to obtain axially uniform deposits. Moreover the influence of unspecific gas admixtures to the reactive gases or change of the anode geometry on reaction rate and static profile was clearly demonstrated and can be exploited for dc glow discharge activated CVD optimization.

References

[1] G.Gärtner, P.Janiel, H.Lydtin: "Plasma-activated CVD of Tungsten/Thorium Structures", Proc.6th Europ.Conf.on CVD, Jerusalem 1987, 319-327

[2] G.Gärtner, P.Janiel, H.Lydtin: "Plasma-activated CVD of Metallic Multicomponent Systems: Th/W PCVD", Proc. of the 6th Int. Conf. on Ion and Plasma Assisted Techniques, Brighton 1987, 17 - 22

[3] F.Weling :"A model for the plasma-activated chemical vapor deposition process" J.Appl.Phys. **57** (9), (1985), 4441 - 4446

[4] F.Weling :"A theoretical description of the PCVD process", Proc. 7th Int. Symp. on Plasma Chemistry, Eindhoven 1985, 165 - 170, Ed. J.Timmermans

[5] D.Küppers and H.Lydtin, Topics in Current Chemistry (Springer, Berlin, Heidelberg), (1980) Vol.89,107 f.

[6] P.K.Bachmann, P.Geittner, H.Lydtin: " Progress in the PCVD Process", Conf.on Opt. Fibre Comm., Atlanta 1986, Techn.Digest A1, 76 - 78.

[7] G.Dittmer, Philips Forschungslabor Aachen, Internal Report, (1987)

[8] S.Vepřek :"Chemical Evaporation and Deposition of Solids in a Non-Isothermal Plasma; Chemical Transport of Carbon", J.Cryst.Growth **17**,(1972), 101 - 116.

Table I: Experimental Parameters of Static PCVD Profiles

Deposition:	W-PCVD	W-PCVD	Th/W-PCVD	Th-PCVD
Fig. No.	3	4	5	6
$P\ [mbar]$:	8	8	5.7	5.8
$T\ [K]$:	640	640	640	640
$\dot{Q}\ (WF_6)\ [sccm]$	64.15	68	27.15	--
$\dot{Q}\ (H_2)\ [sccm]$	375.26	365	277.16	--
$\dot{Q}\ (Ar)\ [sccm]$	326.47	322	442.07	399.85
$\dot{Q}\ (Th(tfa)_4)\ [sccm]$	--	--	1.601	2.08
$\dot{Q}\ (O_2)\ [sccm]$	--	--	64.30	91.92
Plasma Power $\bar{P}_{pl}\ [Watt]$	280	310	230 W	107 W
Discharge Current $I_{pl}\ [A]$	0.5 A	0.5 A	0.45 A	0.3 A
Deposition time t [min]	30 min	21.83 min	30 min	80 min
Efficiency	87.6 %	72 %	99 %	100 %
$a_{eff}\ [cm]$	1.417	1.315	1.417	1.417
$z_A\ [cm]$	6.05	6.05	10.6 cm	10.3 cm
$v\ [cm/s]$	600.7	688	894.2	534.26
$n_{\tilde{A}}\ [cm^{-3}]$	$7.626\ 10^{15}$	$8.2\ 10^{15}$	WF_6: $2.168\ 10^{15}$	--
	--	--	$Th(tfa)_4$: $1.279\ 10^{14}$	$2.780\ 10^{14}$

Table II: Profile Fit Results (*) and Fit-Parameters:

Deposition:	W-PCVD	W-PCVD	*Th*/*W* PCVD (W-content)	*Th*/W-PCVD ($ThO_x F_y$ – content)	Th-PCVD
Fig. No.:	3	4	5a	5b	6
$D\ [cm^2/\ sec]$	473.4	429.9	466.5	176.4	96.72
Plasma length $L\ [cm]$	10 cm	8 cm	5 cm	9 cm	17 cm
Shift z_o (*) $[cm]$	5.97	5.44	12.95	5.87	9.025
Decay length $[cm]$ (*)	21.43	22.24	13.04	24.0	6.78
Rate constant $k\ [s^{-1}]$ (*)	$64.53\ s^{-1}$	$71.23\ s^{-1}$	$157.9\ s^{-1}$	$85.78\ s^{-1}$	$181.4\ s^{-1}$
Peclet number Pe	1.798	2.105	2.716	7.18	7.83
Damköhler number K (*)	0.274	0.287	0.680	0.98	3,77
Number of data points N	20	33	30	33	32
Assigned variance of profile values $[\mu m]$	$2\ \mu m$	$2\ \mu m$	$2\ \mu m$	$0.5\ \mu m$	$2\ \mu m$
X^2_{red} (*)	21.9	3.94	8.84	1.34	5.73
Calculated efficiency (*)	76.4 %	49.5 %	100%	80.7 %	81.2 %
$R_2 R_3$:	H_2	H_2	H_2	O_2	O_2
$n_{R_2 R_3}\ [cm^3]$	$4.461 \cdot 10^{16}$	$4.357 \cdot 10^{16}$	$2.213 \cdot 10^{16}$	$5.137 \cdot 10^{15}$	$1.229 \cdot 10^{16}$
Bimolecular reaction rate constant $k_0\ [cm^3/s]$ (*) :	$1.447 \cdot 10^{-15}$	$1.635 \cdot 10^{-15}$	$7.135 \cdot 10^{-15}$	$1.670 \cdot 10^{14}$	$1.476 \cdot 10^{-14}$

Fig. 1

PCVD-reactor

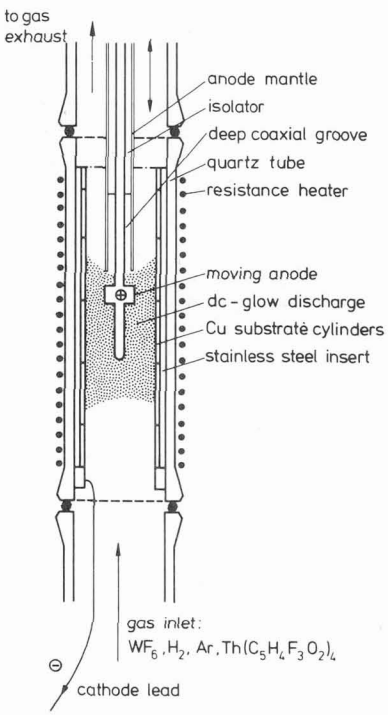

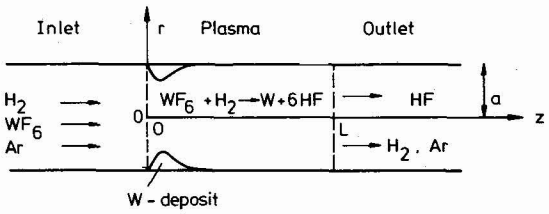

Fig. 2 Schematic view of the W-PCVD-process

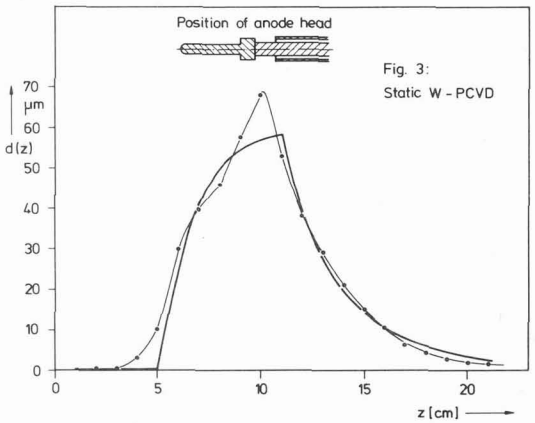

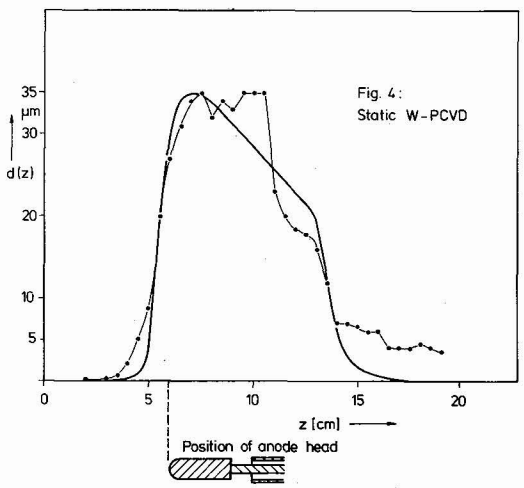

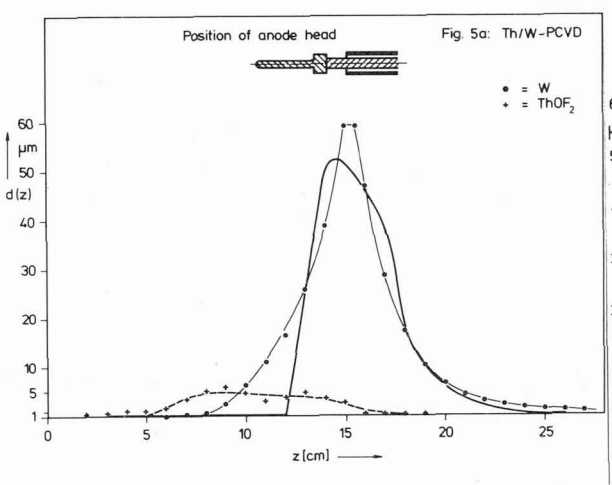
Position of anode head
Fig. 5a: Th/W-PCVD
• = W
+ = $ThOF_2$
d(z)
µm
z [cm]

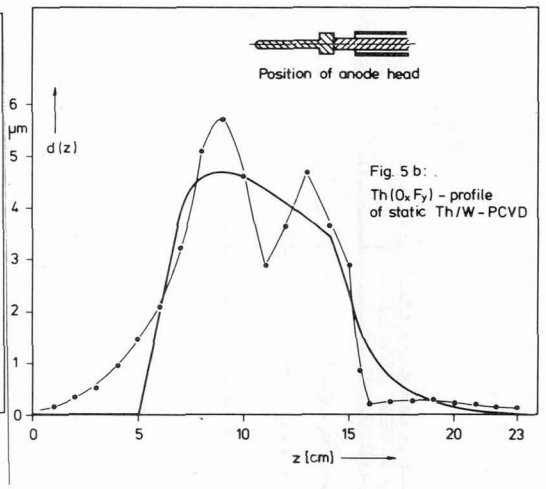
Position of anode head
Fig. 5 b:
$Th(O_xF_y)$ - profile
of static Th/W-PCVD
d(z)
µm
z [cm]

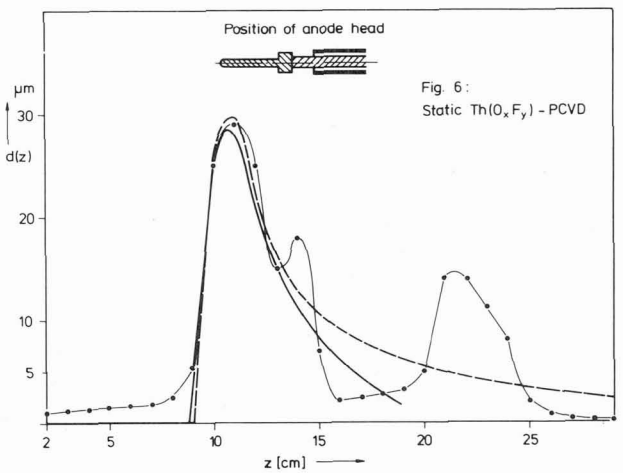
Position of anode head
Fig. 6:
Static $Th(O_xF_y)$ - PCVD
µm
d(z)
z [cm]

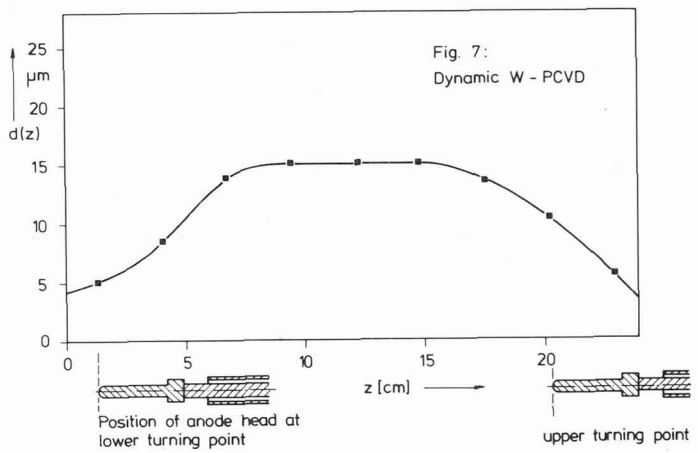
Fig. 7:
Dynamic W - PCVD
µm
d(z)
z [cm]
Position of anode head at
lower turning point
upper turning point